# Negotiation of Intracellular Membrane Barriers by TAT-Modified Gold Nanoparticles

**ARTICLE** *in* ACS NANO · MAY 2011

Impact Factor: 12.88 · DOI: 10.1021/nn201369k · Source: PubMed



**6 AUTHORS**, INCLUDING:

Ian A Prior
University of Liverpool
**87** PUBLICATIONS **4,406** CITATIONS
SEE PROFILE

Violaine Sée
University of Liverpool
**44** PUBLICATIONS **1,764** CITATIONS
SEE PROFILE

# Negotiation of Intracellular Membrane Barriers by TAT-Modified Gold Nanoparticles

Željka Krpetić,[†,#] Samia Saleemi,[†,⊥,#] Ian A. Prior,[‡] Violaine Sée,[§] Rumana Qureshi,[⊥] and Mathias Brust[†,*]

[†]Centre for Nanoscale Science, Department of Chemistry, University of Liverpool, Crown Street, Liverpool L69 7ZD, United Kingdom, [‡]The Physiological Laboratory, Institute of Translational Research, University of Liverpool, Liverpool L69 3BX, United Kingdom, [§]Centre for Cell Imaging, Institute of Integrative Biology, University of Liverpool, Liverpool L69 7ZB, United Kingdom, and [⊥]Electrochemistry Group, Department of Chemistry, Quaid-i-Azam University, Islamabad, P.O. Box 45320, Pakistan. [#]These authors contributed equally to this work.

**ABSTRACT** This paper contributes to the debate on how nanosized objects negotiate membrane barriers inside biological cells. The uptake of peptide-modified gold nanoparticles by HeLa cells has been quantified using atomic emission spectroscopy. The TAT peptide from the HIV virus was singled out as a particularly effective promoter of cellular uptake. The evolution of the intracellular distribution of TAT-modified gold nanoparticles with time has been studied in detail by TEM and systematic image analysis. An unusual trend of particles disappearing from the cytosol and the nucleus and accumulating massively in vesicular bodies was observed. Subsequent release of the particles, both by membrane rupture and by direct transfer across the membrane boundary, was frequently found. Ultimately, near total clearing of particles from the cells occurred. This work provides support for the hypothesis that cell-penetrating peptides can enable small objects to negotiate membrane barriers also in the absence of dedicated transport mechanisms.

**KEYWORDS:** gold nanoparticles · cellular uptake · cell-penetrating peptides · TAT · intracellular trafficking · endosomal escape · transmission electron microscopy

The interactions of nanoparticulate matter with biological systems, especially on the cellular and subcellular level, are currently of great interest for a number of different reasons. Semiconductor and metal nanoparticles have already demonstrated a huge potential as optical probes for research purposes and may become equally important for bioanalytical and diagnostic applications.[1−4] In addition, a broad range of nanoparticles are presently being investigated as agents for the targeted delivery of drugs or genes,[5−9] and there is a significant research effort on developing nanoparticles for hyperthermia and/or photochemical therapies of cancer.[10−17] Finally, the potential toxicity of nanometric objects is an important current concern,[18−21] which can also be addressed by a better understanding of how nanoparticles interact with biological systems. At present, there are no general models with satisfactory predictive power on how nanoparticles are metabolized based on parameters such as their size, shape, chemical composition, charge, and surface functionality. Our knowledge of these phenomena is still at a stage of information gathering, and it appears that even very simple systems, such as well-known cell lines incubated with standard gold nanoparticles, can display a plethora of scenarios, owing to the ability of any biological system to react to external and internal stimuli with a complex response.[22−24] A widely accepted view is that most nanoparticles are taken up by cells via endocytosis and generally remain confined to the system of endocytic vesicles until they are eventually cleared by exocytosis.[25,26]

If there were no alternatives to this trafficking route, the potential usefulness of nanoparticles as intracellular probes and/or agents would be limited, since the particles would never participate in any cytosolic or organelle-based events, except for those occurring within the vesicles to which they are confined. Fortunately, there is increasing evidence for a number of alternative mechanisms that involve the ability of the nanoparticles to enter the cytosol and to overcome membrane boundaries in order to escape from vesicles or to enter specific organelles.[16−20,27] It has previously been demonstrated that so-called cell-penetrating peptides (CPPs) can be used to allow gold nanoparticles to some extent to enter the cytosol and a number of organelles including the nucleus.[27]

Here we report in detail on the intracellular trafficking of gold nanoparticles modified with CPPs, in particular, the TAT sequence from the HIV virus, in HeLa cells. This study focuses on the fate of the particles inside the cell and their ability to overcome intracellular boundaries. Contrary to what has been established for most other

* Address correspondence to M.Brust@liverpool.ac.uk.

Received for review April 13, 2011 and accepted May 24, 2011.

**Published online May 25, 2011**
10.1021/nn201369k

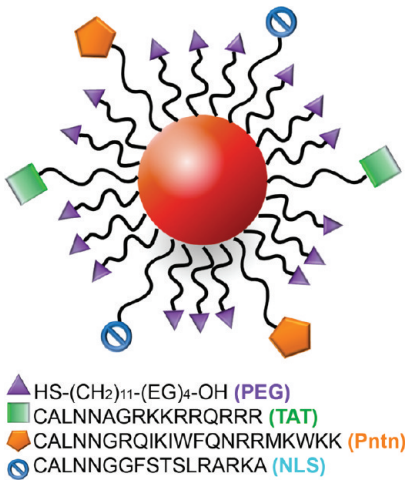


**Figure 1. Schematic representation of a mercaptoethylene glycol-stabilized and peptide-functionalized gold nanoparticle, along with the structure and the amino acid sequences of the ligands. The proportion of peptides in the ligand shell is typically around 5%.**

endocytosed matter, these particles are initially found to be roaming freely in the cytosol and are even able to enter the nucleus and the mitochondria. Only later they are predominantly found in vesicles, from which they are able to escape both by penetration of the vesicle membrane and by membrane rupture. Hence, in this case, the general model of initial confinement to endocytic vesicles followed by the possibility of endosomal escape is not confirmed by our observations.

## RESULTS AND DISCUSSION

Citrate-stabilized gold nanoparticles of 14 ± 1.3 nm (see Supporting Information) were prepared by a modified Turkevich–Frens method[28,29] and subsequently further stabilized and functionalized by a shell of thiolated ligands containing chiefly 11-mercaptoundecyl-tetra(ethylene glycol) (PEG) plus a small amount of a mixture of oligopeptide sequences based on elongations of the standard stabilizing pentapeptide CALNN.[30] A typical multifunctional particle of this type and the amino acid sequences of the peptides utilized for the stabilization are illustrated schematically in Figure 1. Initially, gold nanoparticles containing in the ligand shell a maximum of 6 mol % in total of three different CALNN-based peptides, TAT, Pntn, and NLS, were prepared. This corresponds to approximately 150 to 200 functional peptide ligands on each particle. These are average numbers based on the composition of the solution used to attach the ligand shell. TAT[31] and Pntn[32] are cell-penetrating peptides derived from the HIV virus and *Drosophila*, respectively, while NLS is a well-known nuclear localization sequence.[33] These particles were added to cultures of HeLa cells, a commonly used human fibroblast epithelial cell line, and the total gold content of the cells was determined by atomic emission spectroscopy (AES) after different

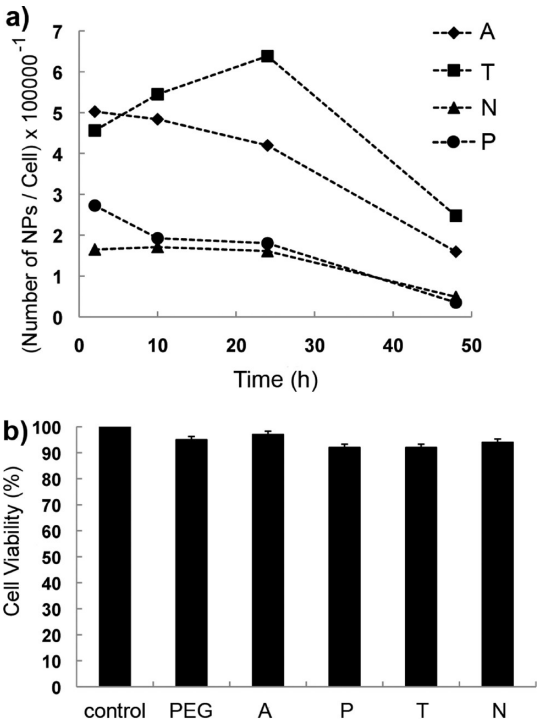


**Figure 2. (a) Intracellular gold content determined by AES as a function of incubation time with differently functionalized gold nanoparticles where A = 2 mol % each of TAT, NLS, and Pntn and 94 mol % of PEG (–♦–), T = 5 mol % of TAT and 95 mol % of PEG (–■–), N = 5 mol % of Pntn and 95 mol % of PEG (–▲–), and P = 5 mol % of NLS and 95 mol % of PEG (–●–). (b) HeLa cell viability determined by MTS assay for A, P, N, T, and PEG particles after 48 h of incubation. No toxicity was found within the time scale of this experiment.**

incubation times. The concentration of the gold nanoparticles in the medium surrounding the cells was 6 nM at all times. The results of these experiments are shown in Figure 2 along with those of toxicity studies using the well-established MTS assay, which measures the respiratory activity of the cells. Importantly, over the duration of this experiment none of the peptide combinations showed significant toxicity, while the extent of cellular uptake in each case was vastly different. There was no indication of any effects the particles might have on cell metabolism or proliferation. With the exception of nanoparticles modified with TAT only, a general trend was observed, according to which from two hours of incubation onward the number of particles per cell decreased slowly with increasing incubation time. This can be only partly explained by the cell multiplication rate that is gradually increasing with time and may eventually outperform the rate of nanoparticle uptake (for details see Supporting Information). Even if this is not taken into account, after two hours of incubation, there is no longer a significant increase in the total amount of gold taken up by the cells. Thus there appears to be a mechanism by which the cells after some time of exposure either limit the uptake of nanoparticles, possibly as a consequence of exhausting their ability to maintain the initial high rate of endocytosis, or enhance

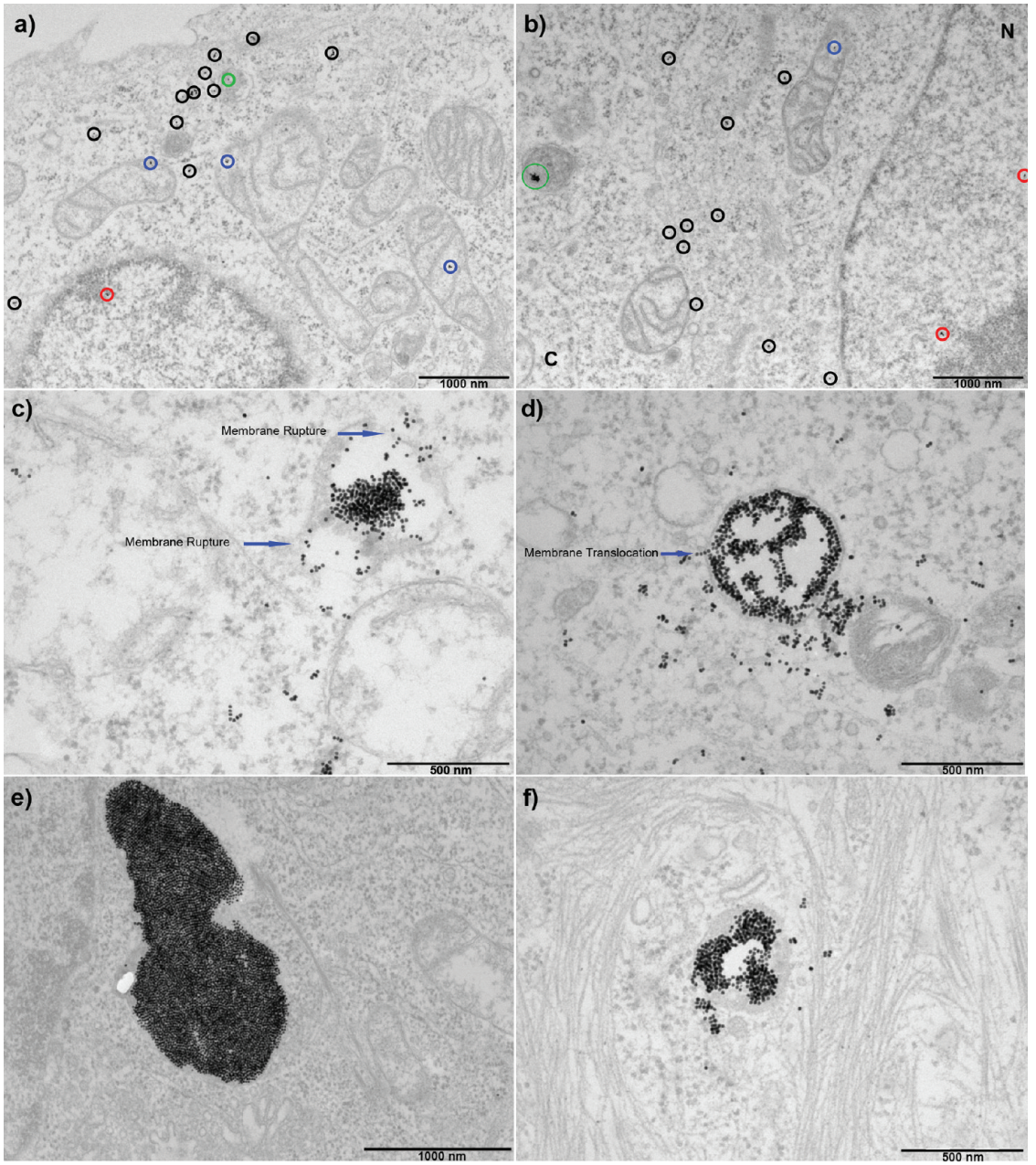


**Figure 3. TEM images of HeLa cells incubated for different times with TAT-modified gold nanoparticles: 2 h incubation showing particles in the cytoplasm (black circles), in mitochondria (blue circles), in the nucleus (red circles), and in vesicles (green circles) (a), a similar scenario but in addition vesicles containing a larger number of particles are found (green circle) after 10 h (b), densely filled vesicle found after 24 h, releasing particles by membrane rupture (c) and by direct membrane translocation (d), and massively packed vesicles found after 24 h (e) and after 48 h (f).**

the rate of nanoparticle clearance by exocytosis. This requires further investigation. The particles modified with TAT only, on the other hand, led to the maximum gold content per cell much later, *i.e.*, after 24 h of incubation. Assuming a homogeneous distribution of the particles inside the cells *i.e.*, not taking into account their compartmentalization, the average intracellular concentration of nanoparticles per cell after 24 h was 0.1 nM. This exceeds the maximum gold content we achieved with any other ligand combination by 30%. For this reason, all further studies were conducted exclusively with particles modified with TAT only. The results of the transmission electron microscopy (TEM) studies after incubation with these particles for different lengths of time are shown in Figures 3 and 4. Also see Supporting Information for a gallery of representative TEM images in support of our claims. After two hours, the shortest incubation time that allowed us to obtain robust AES data to measure the total amount of gold taken up by the cells, practically all internalized particles were found to be located in the cytosol, the nucleus, and the mitochondria, with an overwhelming excess of particles in the cytosol (Figure 3a).

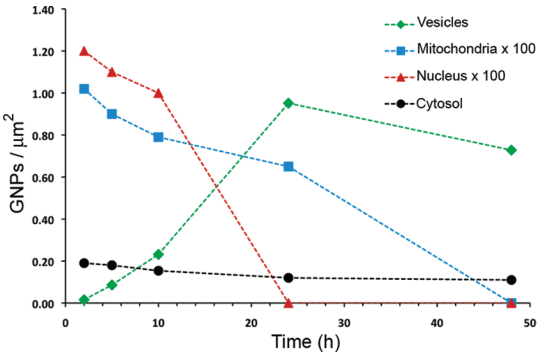


**Figure 4. Evolution of the gold nanoparticle area density at different intracellular locations with time, as determined by stereological analysis of TEM images. See Supporting Information for an example of this procedure.**

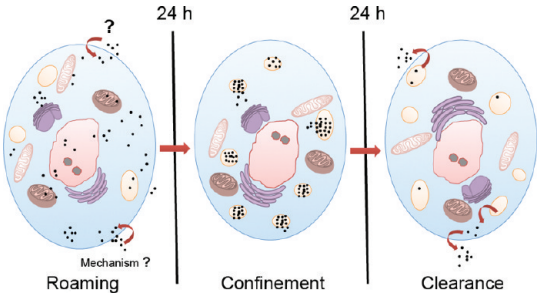


**Figure 5. Scheme illustrating a hypothetical rationalization of the experimental findings summarized in Figure 4. Particles are initially present in the cytosol, the nucleus, and the mitochondria and later become reversibly associated with endolysosomic vesicular bodies perhaps involving a new trafficking pathway. Ultimately, near 100% clearing occurs.**

Only occasionally particles did appear to be present in endocytic vesicles. This is a very surprising finding, which contrasts the behavior of similar particles that have not been modified with CPPs, recently reported in great detail by Rothen-Rutishauser and co-workers[25] for the case of human alveolar epithelial cells. Their findings indicate predominant localization of the particles in vesicles of different sizes with only very few residual particles in the cytosol. This is congruent with the widely accepted view that cellular uptake of nanosized objects occurs exclusively by endocytic mechanisms.[33,34] Our findings, perhaps in contrast, suggest that the presence of TAT on the particle surface enables either rapid escape of particles from the endocytic system or direct translocation of the particles across the plasma membrane, or indeed both. It is also remarkable that particles are found in the nucleus and in the mitochondria. While uptake of positively charged particles by the nucleus through 30 nm pores is not uncommon,[35−37] entering the mitochondria requires the translocation of the particle across a double membrane barrier that is not equipped with uptake mechanisms for objects of the size of these particles. We previously reported similar observations also after 2 h of incubation with CPP-modified gold nanoparticles but were unable to conclude unequivocally that such particles are indeed able to negotiate intracellular membrane barriers.[27] The present study provides more clarity by looking at the subsequent intracellular distribution of the particles with progressing time as quantified in Figure 4. The data presented here are the result from a detailed analysis of a large number of images. For up to 10 h of incubation, the two-hour scenario does not qualitatively change significantly, except for finding fewer particles in the mitochondria and in the nucleus and more in vesicles, where the area density of particles is now higher than in the cytosol (Figure 3b and for 5 h scenario see Supporting Information). A remarkable change is observed after an incubation time of 24 h. Now, particles are no longer found in the nucleus, while the area density of particles in vesicles has increased dramatically. For the first time, massively filled vesicular structures are observed (Figure 3e), which would support the assumption that recruitment of particles from the cytosol into these vesicles can occur. This, however, would represent a very unusual trafficking route of unknown mechanism, for which additional experimental evidence is still absent. An alternative explanation is that, after an initial time of low endocytic activity, an increased uptake of particles by endocytosis is responsible for the formation of these densely filled vesicles. The uncertainties about the entry mechanisms apart, the escape of particles from these vesicles is frequently observed. We present here direct TEM evidence for this process, which can occur both by membrane rupture (Figure 3c) and by direct translocation across the membrane (Figure 3d). At this stage, there appears to be a dynamic exchange of particles between vesicles and the cytoplasm, which we attribute to the presence of the TAT functionality that enables the particles to escape from vesicular structures. After 48 h incubation (Figure 3f) the situation remains practically unchanged, except that particles are no longer found in the mitochondria, and the total amount of particles per cell has decreased by approximately 50% (see Figure 4). The latter we attribute to clearing, presumably by exocytosis. In support of this hypothesis, a chase experiment was conducted in which after 24 h of incubation the particles in the medium were removed, and fresh medium without particles was added. After another 24 h, inspection by TEM established that virtually no particles remained in the cells (see Supporting Information). Within the scope of the present study, we prefer not to speculate about the predominant uptake mechanisms, which would require the availability of data at the very early stage of the incubation period. Such work is in hand. Instead, we focus on the trafficking of particles once they are inside the cell and report their remarkable ability to transfer across membranes of mitochondria and vesicles and the nuclear envelope seemingly without much resistance. A simplified hypothetical scheme summarizing our findings is presented in Figure 5. The salient features of this scheme are (a) the massive

recruitment of nanoparticles into vesicles occurring between 10 and 24 h of incubation time and (b) the subsequent release of particles from these vesicles by at least two different mechanisms as described above. A surprising finding that cannot yet be explained satisfactorily is the observation that only relatively early on particles are found in the nucleus and in the mitochondria. Since the cells remain surrounded by the nanoparticle solution at all times, we would expect to always find some particles at this stage in their trafficking path, even after long incubation times. Seemingly this is not the case, which indicates either that the cells gradually adapt to the presence of the particles and block access to the nucleus and the mitochondria or that the particles lose the ability to reach these organelles as a consequence of a particle aging process. To exclude the latter, we have incubated cells for 24 h with a batch of particles, which was subsequently retrieved and used again to incubate fresh cells for two hours. The results shown in the Supporting Information are identical to those obtained after two-hours incubation with freshly prepared particles. Therefore, potential particle aging is not responsible for the observed inability of particles to enter the nucleus and the mitochondria after prolonged incubation. The absence of particles in the nucleus after 24 h may also partly be due to the enhanced mitotic activity observed at this stage (see Figure S5 in the Supporting Information), during which the nuclear envelope temporarily disappears, so that the release of particles from the dissolved nucleus into the cytosol may be faster than the reuptake of particles by the intact nuclei of the daughter cell generation.

## CONCLUSIONS

We have demonstrated that the modification of gold nanoparticles with the cell-penetrating peptide TAT enhances uptake by HeLa cells and leads to the development of an unusual distribution pattern, by which particles are initially found in the cytosol, the nucleus, and the mitochondria and later within densely filled vesicles, from which they can be released again. Once inside the cell, these particles appear to negotiate intracellular membrane barriers quite freely, including the possibility of direct membrane transfer. Ultimately, in the absence of extracellular nanoparticles, the gold is completely cleared from the cells. Our findings are of importance for all areas in which the trafficking of intracellular nanoparticles is of interest. This includes imaging, drug and gene delivery, nanotoxicology, and the potential therapeutic applications of nanoparticles.

## MATERIALS AND METHODS

**Gold Nanoparticles.** Gold nanoparticles of 14 ± 1.3 nm diameter have been prepared by quickly mixing a boiling solution of 30 mg (0.8 $\mu$mol) of $HAuCl_4$ trihydrate in 300 mL of Milli-Q water with 9 mL of a warm (60−70 °C) 1 wt % aqueous solution of trisodium citrate, followed by reflux for 50 min.[28,29] The mixture was then allowed to cool to room temperature and stirred overnight. The resulting suspension of nanoparticles was filtered using a 0.45 $\mu$m Millipore filter before use. Particles were characterized by UV−vis spectroscopy, TEM, and analytical centrifugation (CPS).

**Functionalization of Gold Nanoparticles.** The modification of the filtered gold nanoparticles with peptides and PEG ligands was carried out following a procedure described by Levy *et al.*[30] For this purpose, 11-mercaptoundecyl-tetra(ethylene glycol) (PEG) was dissolved in methanol to give a 0.1 M stock solution. Peptides were each dissolved in water to give stock solutions of concentrations varying from 0.5 to 0.7 mM, which were frozen and stored at −20 °C. Methanolic PEG and aqueous peptides were mixed in the desired proportions to give a total volume between 100 and 200 $\mu$L. This was then added quickly under vigorous stirring to the aqueous suspension of nanoparticles. In total, always 410 nmol of premixed ligands was added to 10 mL of a 2 nM gold nanoparticle suspension. After allowing the ligands to attach to the nanoparticles overnight, the particles were cleaned by repeated centrifugation and redispersion in water (three times). Before use, these particles were filtered by centrifugation using Ultrafree-MC GV 0.22 $\mu$m (sterile).

**Cell Culture.** HeLa cells (American Culture Collection) were cultured in Dulbecco's modified Eagle medium containing 10% fetal bovine serum (FBS) and 1% each of nonessential amino acid solution and penicillin−streptomycin in 3 cm culture dishes at 37 °C in a humidified atmosphere containing 95% air and 5% $CO_2$ (v/v). Before incubation with gold nanoparticles this medium was removed by aspiration, and the cells were washed twice with PBS (1 × DPBS, Gibco, Dulbecco). Then, 2 mL of a 6 nM suspension of gold nanoparticles in fresh medium of the same formulation was added, and the cells were incubated for the desired time under the above conditions. Cells were 80% confluent at the time of processing for TEM.

**Transmission Electron Microscopy.** After incubation, the medium containing the excess nanoparticles was removed and the cells were washed three times with PBS. Primary fixation of the cells was carried out with a 0.1 M PBS solution of 4% paraformaldehyde and 2.5% glutaraldehyde for 1 h. The cells were then washed with PBS and postfixed using a 1% aqueous solution of $OsO_4$ (caution: extremely toxic!) for 1 h followed by successive washings with PBS, water, and 30% ethanol. Staining with 0.5% uranyl acetate (0.5 mL, in 30% ethanol) was carried out for 1 h. Cells were then dehydrated using increasing concentrations of ethanol (30%, 60%, 70%, 80%, and 100%). Finally the cell pellets were infiltrated first with a mixture of 1:1 epoxy resin in 100% ethanol and then with the resin only and were left to polymerize at 60 °C for 48 h. Ultrathin sections (~70−100 nm) were cut using a Leica Ultramicrotome using a diamond knife. Formvar-coated copper grids with sections mounted on them were stained with 5% uranyl acetate in 50% ethanol and 2% aqueous lead citrate solution and imaged using a FEI Tecnai Spirit TEM at 100 kV.

**Image Analysis.** AnalySIS software (Soft Imaging Systems) was used to manipulate and analyze images and particle uptake at subcellular levels. Nanoparticle subcellular locations were counted using a stereological sampling approach. Briefly, a box pattern was overlaid over each image and each square was scored for nanoparticle content and subcellular location. These were then integrated with the image magnification to give nanoparticle counts per square micrometer. At least 200 to 300 boxes in 25−30 images were counted for each condition. Approximately 7−10 cells were imaged per condition. Images have been selected randomly from a set of images recorded for different experiments. All experiments were performed on average three times and were highly reproducible. Statistical

information about data obtained to develop Figure 4 is shown in the Supporting Information.

**Determination of Gold Content.** Cells were incubated for 2, 10, 24, and 48 h with a concentration of 6 nM CPP-functionalized gold nanoparticles in 3 cm dishes and were subsequently washed five times with PBS in order to remove excess gold nanoparticles. In order to detach the cells from the dish, 1 mL of an aqueous trypsin (Gibco 0.05%) solution was added, and the detached cells were rinsed out with 2 mL of water and collected in a glass vial carefully avoiding any loss. To this was added 5 mL of *aqua regia* (caution: extremely corrosive), and the mixture was left for 72 h, leading to the complete dissolution of all cellular material. The samples were diluted with water to a final volume of 16 mL before the intracellular amount of gold was determined by ICP-AES (Spectro Ciros CCD). Cells were counted manually using a hemacytometer after trypsinization, for each time of incubation. Standard solutions of gold for calibration were purchased from Aldrich and diluted with the same matrix used for the samples.

**Cell Proliferation Assay.** A cell proliferation test was carried out using a colorimetric MTS assay. Cells were cultured at a density of $5 \times 10^3$ cells per 100 $\mu$L per well in a flat-bottomed 96-well plate in MEM medium with 10% FBS and 1% each of nonessential amino acid solution at 37 °C in a humidified atmosphere containing 95% air and 5% $CO_2$ (v/v). One day after plating, cells were incubated with the nanoparticles for 48 h. At the end of the incubation period CellTiter 96 Aqueous One solution (Promega, Madison, WI, USA) was added, and the mixture was incubated 2 h at 37 °C according to the manufacturer's instructions. The optical densities were assessed with a plate reader at 492 nm.

*Acknowledgment.* The authors wish to thank Alison Beckett for TEM assistance and George Miller for the AES measurements. Partial financial support from the Higher Education Commission (HEC) of Pakistan is greatly acknowledged (S.S. and R.Q.).

*Supporting Information Available:* Determination of gold content taken up by HeLa cells by AES; gallery of representative images showing TAT-modified gold nanoparticles in HeLa cells at different incubation times (2, 5, 10, 24, and 48 h); characterization of gold nanoparticles. This material is available free of charge *via* the Internet at http://pubs.acs.org.

## REFERENCES AND NOTES


1. Sée, V.; Free, P.; Cesbron, Y.; Nativo, P.; Shaheen, U.; Rigden, D. J.; Spiller, D. G.; Fernig, D. G.; White, M. R. H.; Prior, I. A.; *et al*. Cathepsin L Digestion of Nanobioconjugates upon Endocytosis. *ACS Nano* **2009**, *3*, 2461–2468.
2. Luccardini, C.; Yakovlev, A.; Gaillard, S.; Van't Hoff, M.; Alberola, A. P.; Mallet, J. M.; Parak, W. J.; Feltz, A.; Oheim, M. Getting Across the Plasma Membrane and Beyond: Intracellular Uses of Colloidal Semiconductor Nanocrystals. *J. Biomed. Biotechnol.* **2007**, *2007*, 1–9.
3. Parak, W. J.; Pellegrino, T.; Plank, C. Labelling of Cells with Quantum Dots. *Nanotechnology* **2005**, *16*, R9–R25.
4. Alivisatos, A. P.; Gu, W. W.; Larabell, C. Quantum Dots as Cellular Probes. *Annu. Rev. Biomed. Eng.* **2005**, *7*, 55–76.
5. Kim, C.; Agasti, S. S.; Zhu, Z. J.; Isaacs, L.; Rotello, V. M. Recognition-Mediated Activation of Therapeutic Gold Nanoparticles Inside Living Cells. *Nat. Chem.* **2010**, *2*, 962–966.
6. Sandhu, K. K.; McIntosh, C. M.; Simard, J. M.; Smith, S. W.; Rotello, V. M. Gold Nanoparticle-Mediated Transfection of Mammalian Cells. *Bioconjugate Chem.* **2002**, *13*, 3–6.
7. Koo, O. M.; Rubinstein, I.; Onyuksel, H. Role of Nanotechnology in Targeted Drug Delivery and Imaging: a Concise Review. *Nanomed.-Nanotechnol.* **2005**, *1*, 193–212.
8. Vega, R. A.; Wang, Y.; Harvat, T.; Wang, S. S.; Qi, M.; Adewola, A. F.; Lee, D.; Benedetti, E.; Oberholzer, J. Modified Gold Nanoparticle Vectors: A Biocompatible Intracellular Delivery System for Pancreatic Islet Cell Transplantation. *Surgery* **2010**, *148*, 858–865.
9. Avnesh, K.; Kumar, Y. S. Cellular Interactions of Therapeutically Delivered Nanoparticles. *Expert Opin. Drug Delivery* **2011**, *8*, 141–151.
10. Choi, W. I.; Kim, J.-K.; Kang, C.; Byeon, C. C.; Kim, Y. H.; Tae, G. Tumor Regression in Vivo by Photothermal Therapy Based on Gold-Nanorod-Loaded, Functional Nanocarriers. *ACS Nano* **2011**, *5*, 1995–2003.
11. Huang, X. H.; Jain, P. K.; El-Sayed, I. H.; El-Sayed, M. A. Plasmonic Photothermal Therapy (PPTT) Using Gold Nanoparticles. *Lasers Med. Sci.* **2008**, *23*, 217–228.
12. Nam, J.; Won, N.; Jin, H.; Chung, H.; Kim, S. pH-Induced Aggregation of Gold Nanoparticles for Photothermal Cancer Therapy. *J. Am. Chem. Soc.* **2009**, *131*, 13639–13645.
13. El-Sayed, I. H.; Huang, X. H.; El-Sayed, M. A. Selective Laser Photo-Thermal Therapy of Epithelial Carcinoma Using Anti-EGFR Antibody Conjugated Gold Nanoparticles. *Cancer Lett.* **2006**, *239*, 129–135.
14. Hainfeld, J. F.; Slatkin, D. N.; Smilowitz, H. M. The Use of Gold Nanoparticles to Enhance Radiotherapy in Mice. *Phys. Med. Biol.* **2004**, *49*, N309–N315.
15. Bartczak, D. M. O. L.; Millar, T. M.; Sanchez-Elsner, T.; Kanaras, A. G. Laser-Induced Damage and Recovery of Plasmonically Targeted Human Endothelial Cells. *Nano Lett.* **2011**, *11*, 1358–1363.
16. Huang, X. H.; Kang, B.; Qian, W.; Mackey, M. A.; Chen, P. C.; Oyelere, A. K.; El-Sayed, I. H.; El-Sayed, M. A. Comparative Study of Photothermolysis of Cancer Cells with Nuclear-Targeted or Cytoplasm-Targeted Gold Nanospheres: Continuous Wave or Pulsed Lasers. *J. Biomed. Opt.* **2010**, *15*, 058002-1–058002-7.
17. Krpetić, Ž.; Nativo, P.; Sée, V.; Prior, I. A.; Brust, M.; Volk, M. Inflicting Controlled Nonthermal Damage to Subcellular Structures by Laser-Activated Gold Nanoparticles. *Nano Lett.* **2010**, *10*, 4549–4554.
18. Krug, H. F.; Wick, P. Nanotoxicology: An Interdisciplinary Challenge. *Angew. Chem., Int. Ed.* **2011**, *50*, 1260–1278.
19. Maynard, A. D.; Warheit, D. B.; Philbert, M. A. The New Toxicology of Sophisticated Materials: Nanotoxicology and Beyond. *Toxicol. Sci.* **2010**, *120*, S109–S129.
20. Arnida; Malugin, A.; Ghandehari, H. Cellular Uptake and Toxicity of Gold Nanoparticles in Prostate Cancer Cells: a Comparative Study of Rods and Spheres. *J. Appl. Toxicol.* **2010**, *30*, 212–217.
21. Ikah, D. S. K.; Howard, C. V.; McLean, W. G.; Brust, M.; Tshikhudho, R. Neurotoxic Effects of Monodispersed Colloidal Gold Nanoparticles. *Toxicology* **2006**, *219*, 238–239.
22. Wang, S. H.; Lee, C. W.; Chiou, A.; Wei, P. K. Size-Dependent Endocytosis of Gold Nanoparticles Studied by Three-Dimensional Mapping of Plasmonic Scattering Images. *J. Nanobiotechnol.* **2010**, *8*, 33.
23. Chithrani, D. B. Intracellular Uptake, Transport, and Processing of Gold Nanostructures. *Mol. Membr. Biol.* **2010**, *27*, 299–311.
24. Chithrani, B. D.; Chan, W. C. W. Elucidating the Mechanism of Cellular Uptake and Removal of Protein-Coated Gold Nanoparticles of Different Sizes and Shapes. *Nano Lett.* **2007**, *7*, 1542–1550.
25. Brandenberger, C.; Muhlfeld, C.; Ali, Z.; Lenz, A. G.; Schmid, O.; Parak, W. J.; Gehr, P.; Rothen-Rutishauser, B. Quantitative Evaluation of Cellular Uptake and Trafficking of Plain and Polyethylene Glycol-Coated Gold Nanoparticles. *Small* **2010**, *6*, 1669–1678.
26. Bartczak, D.; Sanchez-Elsner, T.; Louafi, F.; Millar, T. M.; Kanaras, A. G. Receptor-Mediated Interactions between Colloidal Gold Nanoparticles and Human Umbilical Vein Endothelial Cells. *Small* **2011**, *7*, 388–394.
27. Nativo, P.; Prior, I. A.; Brust, M. Uptake and Intracellular Fate of Surface-Modified Gold Nanoparticles. *ACS Nano* **2008**, *2*, 1639–1644.
28. Turkevich, J.; Stevenson, P. C.; Hillier, J. A Study of the Nucleation and Growth Processes in the Synthesis of Colloidal Gold. *Discuss. Faraday Soc.* **1951**, *11*, 55–75.
29. Frens, G. Controlled Nucleation for Regulation of Particle-Size in Monodisperse Gold Suspensions. *Nat.-Phys. Sci.* **1973**, *241*, 20–22.
30. Lévy, R.; Thanh, N. T. K.; Doty, R. C.; Hussain, I.; Nichols, R. J.; Schiffrin, D. J.; Brust, M.; Fernig, D. G. Rational and Combinatorial Design of Peptide Capping Ligands for

Gold Nanoparticles. *J. Am. Chem. Soc.* **2004**, *126*, 10076–10084.
31. de la Fuente, J. M.; Berry, C. C. TAT Peptide as an Efficient Molecule to Translocate Gold Nanoparticles into the Cell Nucleus. *Bioconjugate Chem.* **2005**, *16*, 1176–1180.
32. Lundberg, P.; Langel, U. Uptake Mechanisms of Cell-Penetrating Peptides Derived from the Alzheimer's Disease Associated Gamma-Secretase Complex. *Int. J. Pept. Res. Ther.* **2006**, *12*, 105–114.
33. Tkachenko, A. G.; Xie, H.; Coleman, D.; Glomm, W.; Ryan, J.; Anderson, M. F.; Franzen, S.; Feldheim, D. L. Multifunctional Gold Nanoparticle-Peptide Complexes for Nuclear Targeting. *J. Am. Chem. Soc.* **2003**, *125*, 4700–4701.
34. Krpetić, Ž.; Porta, F.; Caneva, E.; Dal Santo, V.; Scari, G. Phagocytosis of Biocompatible Gold Nanoparticles. *Langmuir* **2010**, *26*, 14799–14805.
35. Wunderbaldinger, P.; Josephson, L.; Weissleder, R. TAT Peptide Directs Enhanced Clearance and Hepatic Permeability of Magnetic Nanoparticles. *Bioconjugate Chem.* **2002**, *13*, 264–268.
36. Santra, S.; Yang, H.; Dutta, D.; Stanley, J. T.; Holloway, P. H.; Tan, W. H.; Moudgil, B. M.; Mericle, R. A. TAT Conjugated, FITC Doped Silica Nanoparticles for Bioimaging Applications. *Chem. Commun.* **2004**, *24*, 2810–2811.
37. Pujals, S.; Bastus, N. G.; Pereiro, E.; Lopez-Iglesias, C.; Puntes, V. F.; Kogan, M. J.; Giralt, E. Shuttling Gold Nanoparticles into Tumoral Cells with an Amphipathic Proline-Rich Peptide. *ChemBioChem* **2009**, *10*, 1025–1031.